JOURNAL OF MAGNETIC RESONANCE **132,** 181–190 (1998)
ARTICLE NO. MN981415

# Efficient Time Propagation Technique for MAS NMR Simulation: Application to Quadrupolar Nuclei

Thibault Charpentier,*,[1] Claude Fermon,* and Joseph Virlet†

*Service de Physique de l'État Condensé and †Service de Chimie Moléculaire, CEA Saclay, 91191 Gif sur Yvette Cedex, France

Received August 7, 1997; revised January 21, 1998

**The quantum mechanical Floquet theory is investigated in order to derive an efficient way of performing numerical calculations of the dynamics of nuclear spin systems in MAS NMR experiments. Here, we take advantage of time domain integration of the quantum evolution over one period as proposed by Eden *et al.* (*1*). But a full investigation of the propagator $U(t, t_0)$, and especially its dependence with respect to $t$ and $t_0$ within a formalized approach, leads to further simplifications and to a substantial reduction in computation time when performing powder averaging for any complex sequence. Such an approximation is suitable for quadrupolar nuclei ($I > 1/2$) and can be applied to the simulation of the RIACT (rotational induced adiabatic coherence transfer) phenomenon that occurs under special experimental conditions in spin locking experiments (*2–4*). The present method is also compared to the usual infinite dimensional Floquet space approach (*5, 6*), which is shown to be rather inefficient. As far as we know, it has never been reported for quadrupolar nuclei with $I \geq 3/2$ in spin locking experiments. The method can also be easily extended to other areas of spectroscopy.** 

*Key Words:* **Floquet theory; MAS simulation; RIACT; quadrupolar nuclei.**

## I. INTRODUCTION

The quantum mechanical Floquet theory is a powerful tool for the description of a quantum system subjected to a periodically time-dependent Hamiltonian. It was first applied to spectroscopy by Shirley (*7*) and is nowadays a subject of great interest because of its ability to provide an efficient way of computing the time-dependent response of the system, such as in laser–molecule interactions (*8–12*) or in NMR. In the latter the spinning of the sample around the magic angle has become a widespread technique and numerous studies using the Floquet theory have been proposed to describe the full spinning sideband pattern using a formalized approach (*13*), rotational resonance phenomena (*14–17*), or the cross polarization process (*18*) and its optimization (*19, 20*). These studies reveal that the Floquet theory is usually applied in its time-independent Hamiltonian approach in NMR spectroscopy. Progress in time propagation technique has been made by Eden *et al.* (*1*), who took advantage of time integration over one period of the quantum evolution to compute directly the Fourier spectrum of the signal. This reduces the calculation time required for long time propagation to the one needed by a inverse Fourier transform. Most of these studies have been done for spin 1/2. Applications of the Floquet theory for nuclei with spin $I > 1/2$ that possess a quadrupole moment $Q$, called quadrupolar nuclei, have received less attention except for the simple case of MAS spectra for FID computation (*13*).

Calculations for description of spin locking experiments (*2, 3, 21*) or nutation experiments (*22–24*) in NMR of quadrupolar nuclei have usually been performed using the recursive method. The Hamiltonian is considered to be constant over a small interval time $\delta t$ and the propagator is approximated as $U(t + \delta t, t) = e^{-iH(t)\delta t}$. The simplicity of this calculation has resulted in its widespread use, but compared to the present approach, this method requires long time propagation and powder averaging. A theoretical model using the Floquet theory for deuterium ($I = 1$) cross polarization MAS (*25*) has been recently reported but the quadrupolar coupling constants involved were relatively small compared to those of typical half-integer nuclei such as $^{23}$Na or $^{27}$Al (of the order of megahertz). For these nuclei, and in the case of strong irradiation (typically 100 kHz), the Floquet space approach fails because an accurate description requires a large number of Fourier components, which makes the method inefficient, whereas the average Hamiltonian approach (*26–28*) widely used for multipulse experiments is devoted to stroboscopic observation.

Thus there is a need for an efficient method for simulating quadrupolar nuclei NMR in a rotating sample in order to investigate new experiments such as multipulse experiments or cross polarization processes between several dipolar coupled nuclei. We propose to illustrate our approach by a description of the RIACT phenomena using our formalism. For such an experiment the crucial dependency upon the offset leads to use high RF power. For comparison, we also introduce the Floquet space in block operator formalism as proposed by Llor (*29*) and use it in our simulations.

The remainder of the paper is organized as follows. In Section II we present the Floquet theorem with a deeper investigation of the propagator $U(t, t_0)$ and the numerical processes used. Section III is devoted to the introduction of the Floquet space in a block operator formalism and to the link between the two approaches,

[1] Fax number: 01.69.08.87.86; e-mail: charpent@spec.saclay.cea.fr.



1090-7807/98 $25.00

especially in computing $U(t, t_0)$. Section IV gives the application to the evolution of an observable and to its averaged signal. It is shown that a formal average over $\gamma$ can be performed for usual Hamiltonians that are continuous and that verify $H(\gamma, t) = H(0, t + \gamma/\omega_R)$, where $\gamma$ is the third component of the Euler angle giving the orientation of the crystallite with respect to the rotor fixed frame. Section V discusses the case of complex sequences such as in multiple pulse techniques. Finally, Section VI gives the application to RIACT.

## II. FLOQUET THEORY REVISITED

We consider a finite quantum spin system subjected to a periodically modulated Hamiltonian

$$H(t) = \sum_m H_m e^{im\omega_R t} \qquad [1]$$

of period $T_R = 2\pi/\omega_R$. An initial state described by the density operator $\rho(t_0)$ evolves according to

$$\rho(t) = U(t, t_0)\rho(t_0)U^+(t, t_0), \qquad [2]$$

where the evolution operator $U(t, t_0)$ is the solution of the Schrödinger equation

$$i\frac{dU(t, t_0)}{dt} = H(t)U(t, t_0), \qquad [3]$$

satisfying $U(t_0, t_0) = \mathrm{Id}$. According to the Floquet theorem (*30*), $U(t, 0)$ can be expanded as the product

$$U(t, 0) = P(t)e^{-i\bar{H}t}, \qquad [4]$$

where $P(t)$ is a unitary $T_R$-periodic operator satisfying $P(T_R) = P(0) = \mathrm{Id}$, and the constant Hermitian operator $\bar{H}$ is the so-called average or effective Hamiltonian. Using the well-known property

$$U(t, t_0) = U(t, 0)U^+(t_0, 0) \qquad [5]$$

and Eq. [4], we obtain the expansion

$$U(t, t_0) = P(t)e^{-i\bar{H}(t-t_0)}P^+(t_0). \qquad [6]$$

It is evident from Eq. [6] that the choice of the average Hamiltonian is not unique. Indeed, for any unitary transformation X, the substitutions $P(t) \Leftarrow P(t)X$ and $\bar{H} \Leftarrow X^+\bar{H}X$ do not change the evolution operator Eq. [6]. If $X$ is chosen as the diagonalizing matrix of $\bar{H}$ ($\bar{\Omega} = X^+\bar{H}X$ and $F(t) = P(t)X$), one gets an expansion similar to that used by Shirley (*7*),

$$U(t, t_0) = F(t)e^{-i\bar{\Omega}(t-t_0)}F^+(t_0), \qquad [7]$$

which, with Eq. [6], will be used for the remainder of the paper. Furthermore, Eq. [7] can be transformed into an expression similar to Eq. [4],

$$U(t, t_0) = F(t)F^+(t_0)e^{-i[F(t_0)\bar{\Omega}F^+(t_0)]t}, \qquad [8]$$

defining a new average Hamiltonian $\bar{H}(t_0) = F(t_0)\bar{\Omega}F^+(t_0)$ which describes a stroboscopic observation with a time shifted by $t_0$ with respect to $\bar{H}$.

Equation [7] is similar to the form obtained by Llor but more general as an arbitrary initial time is introduced. It can be interpreted as follows: $F(t)$ defines a generalized interaction frame where the time-dependent periodic Hamiltonian $H(t)$ is reduced to the time-independent diagonal average Hamiltonian $\bar{\Omega}$. One enters in this frame at time $t_0$, evolves under the time-independent Hamiltonian, and then goes back the initial frame at time $t$. This transformation is in fact very similar to the canonical transformation introduced for the study of the dynamics of spin systems in multipulse experiments (*31*). This point is further discussed later.

For numerical calculation, the advantage of Eq. [7] is to provide the propagator $U(t, t_0)$ for any values of $t$ and $t_0$ from the operators $F(t)$ and $\bar{\Omega}$, which can be deduced from a calculation over a *unique* period of rotation of the propagator $U(t, 0)$. The equations

$$U(T_R, 0) = e^{-i\bar{H}T_R} = F(0)e^{-i\bar{\Omega}T_R}F^+(0) \qquad [9]$$

$$F(t) = U(t, 0)F(0)e^{+i\bar{\Omega}t} \qquad [10]$$

provides $\bar{\Omega}$ and $F(t)$ for $t$ in $[0, T_R]$. Practically, the COMPUTE (*1*) protocol is used by discretizing the period of rotation in $N$ steps of duration $\delta t = T_R/N$. The intermediate propagators $U(t_j, 0)$ for $j$ in $[0, N]$ ($t_j = j\delta t$) are calculated by the approximation

$$U(t_{j+1}, 0) = e^{-iH(t_j+\delta t/2)\delta t}U(t_j, 0), \qquad [11]$$

which is more accurate (*32*) than the usual $U(t_{j+1}, 0) = e^{-iH(t_j)\delta t}U(t_j, 0)$. The Fourier components $F_n$ of $F(t) = \Sigma_n F_n e^{in\omega_R t}$ defined by

$$F_n = \frac{1}{T_R}\int_0^{T_R} U(t, 0)F(0)e^{i\bar{\Omega}t}e^{-in\omega_R t}dt \qquad [12]$$

are numerically obtained for $n$ in $[-N/2 + 1, N/2]$ by

$$F_n = \frac{1}{N}\sum_{j=0}^{N-1} U(t_j, 0)F(0)e^{+i\bar{\Omega}t_j}e^{-in\omega_R t_j}. \qquad [13]$$

This leads to the Fourier expansion of the evolution operator with respect to $t$ and $t_0$,

$$U(t, t_0) = \sum_{m,n} F_m e^{-i\bar{\Omega}(t-t_0)} F_n^+ e^{im\omega_R t} e^{-in\omega_R t_0}. \quad [14]$$

## III. FLOQUET SPACE

Floquet space is often used because it provides an efficient way of dealing with time-dependent problems by lifting the time dependency for an infinite dimension. This has to be naturally truncated in numerical simulations. The formulation we propose in the following can be seen as a way of indirectly calculating the diagonalizing matrix $W^F$ of the Floquet Hamiltonian $H^F$, even when the dimension is large. We briefly introduce the Floquet space method in order to compare it with the method developed in the previous section.

The Floquet Hamiltonian can be introduced (*29*) by inserting the Fourier expansion of $U(t, 0)$, Eq. [14],

$$U(t, 0) = \sum_n F_n e^{-i\bar{\Omega}t} F^+(0) e^{+in\omega_R t} = \sum_n U_n(t) e^{+in\omega_R t} \quad [15]$$

in the Schrödinger equation [3]. $H_F$ is then defined by the set of relations

$$i \frac{dU_n(t)}{dt} = \sum_p H^F_{n,p} U_p(t), \quad [16]$$

where $H^F_{n,p} = H_{n-p} + n\omega_R \delta_{n,p}$ Id are its block matrix elements. The eigenvalues $\bar{\omega}_r$ of $\bar{\Omega}$ being defined mod$[\omega_R]$, the same is true for the diagonal elements of $H^F$, whereas the $U_n(t)$ are defined within a multiplicative factor $e^{ik\omega_R t}$. We choose, as usual, $-\omega_R/2 < \bar{\omega}_r \leq +\omega_R/2$. This defines the $U_n(t)$ in a unique way and makes them ''slowly varying'' as possible.

For notational convenience, we introduce the mode state bases $|n\rangle$ (*13*) whose time representations are $\langle t|n\rangle = e^{in\omega_R t}$. The evolution operator can be then represented by a Floquet wavefunction (*29*)

$$|\Phi^F(t)\rangle = e^{-iH^F t} |\Phi^F(0)\rangle \quad [17]$$

whose components are the operators $U_n(t)$,

$$|\Phi^F(t)\rangle = \begin{pmatrix} \cdots \\ U_0(t) \\ U_1(t) \\ \cdots \end{pmatrix} = \sum_n U_n(t)|n\rangle. \quad [18]$$

Whence, according to Eq. [15],

$$|\Phi^F(0)\rangle = \sum_n F_n F^+(0)|n\rangle. \quad [19]$$

In this block operator formalism, the evolution operator is simply obtained through a $\langle t \mid$ product, that is,

$$\langle t|\Phi^F(t)\rangle = \langle t| \left(\sum_n |n\rangle\langle n|\right) |\Phi^F(t)\rangle = \sum_n \langle n|\Phi^F(t)\rangle e^{in\omega_R t}$$
$$= \sum_n U_n(t) e^{in\omega_R t} = U(t, 0). \quad [20]$$

This leads to the expansion

$$U(t, 0) = \sum_n \langle n|e^{-iH^F t}|\Phi^F(0)\rangle e^{in\omega_R t}, \quad [21]$$

which appears equivalent (see Appendix A) to the usual expression (*25, 33–35*)

$$U(t, 0) = \sum_p \langle p|e^{-iH^F t}|0\rangle e^{ip\omega_R t}. \quad [22]$$

But, here, the Fourier coefficients in Eq. [21] $U_n(t)$ are slow varying in contrast to those in Eq. [22] (see Appendix B).

The relation Eq. [20] also gives the Floquet representation of $U(t, t_0) = U(t, 0)U^+(t_0, 0)$:

$$U(t, t_0)$$
$$= \langle t|\Phi^F(t)\rangle\langle\Phi^F(t_0)|t_0\rangle$$
$$= \sum_{m,n} \langle m|e^{-iH^F t}|\Phi^F(0)\rangle\langle\Phi^F(0)|e^{iH^F t_0}|n\rangle e^{im\omega_R t} e^{-in\omega_R t_0}. \quad [23]$$

Taking $t_0 = 0$ and using $\Sigma_n \langle\Phi^F(0)|n\rangle = \text{Id}$ (Eq. [19]) shows that Eq. [23] is consistent with Eq. [21]. With the aid of the band structure and change in the summation indices (calculations similar to Appendix A), Eq. [23] can be reduced to the formula

$$U(t, t_0) = \sum_m \langle m|e^{-iH^F(t-t_0)}|0\rangle e^{im\omega_R t}, \quad [24]$$

which has been widely used in the context of multiphotonic processes (*8–12*). It can be also transformed into the unusual representation

$$U(t, t_0) = \sum_m \langle 0|e^{-iH^F(t-t_0)}|m\rangle e^{-im\omega_R t_0}, \quad [25]$$

which allows a separation between the evolution duration $t - t_0$ and the initial phase shift $m\omega_R t_0$ of each Floquet mode.

To perform calculations in Floquet space, we use Eq. [20]. Let $W^F$ be the diagonalizing matrix ${}^X H^F (e^{-iH^F t} = W^F e^{-i\Omega^F t} W^{F+})$. As shown in Appendix C, the elements of $W^F$ in the Floquet space are linked to the Fourier components of $F(t)$ through the essential relation

$$F_n = \langle n|W^F|0\rangle = \langle n + p|W^F|p\rangle. \quad [26]$$

Then, if we have an efficient way of evaluating $F(t)$ and $\bar{\Omega}$ (Eq. [7]), the full diagonalization of $H^F$ is unnecessary.

The important result of this section is the link between the Floquet space and the usual recursive approaches which is obtained by comparing the expressions [26] and [12] of $F_n$. The general relation between the two approaches is in fact

$$\langle n|W^F|0\rangle = \frac{1}{T_R}\int_0^{T_R} U(t, 0) F(0) e^{i\bar{\Omega}t} e^{-in\omega_R t} dt. \quad [27]$$

This allows much faster calculations in Floquet space. However, for numerical analysis, the approach of the next section is more efficient and should be preferred.

## IV. EVOLUTION OF AN OBSERVABLE AND POWDER AVERAGING

In solid-state NMR, the Hamiltonian is dependent on the orientation of the tensorial interactions with respect to the magnetic field in the laboratory frame. For powder samples, magic angle spinning (MAS) NMR is used to get high-resolution spectra. This makes the Hamiltonian time-dependent and periodic. Let the orientation of the crystallite in the rotor frame be described by the Euler angle $(\alpha, \beta, \gamma)$. The dependence on the third angle $\gamma$ appears as a time shift $t_\gamma = \gamma/\omega_R$, that is, $H(\alpha, \beta, \gamma, t) = H(\alpha, \beta, 0, t + t_\gamma)$. When performing a powder average over the three Euler angles in order to get the powder spectrum, this allows us to replace the third one by an integration over the time shift $t_\gamma$. In the following, the $(\alpha, \beta)$ dependence is assumed implicitly so that, for instance, one writes $H(\gamma, t)$ for $H(\alpha, \beta, \gamma, t)$.

Let $T$ be the observable. For a spin system with time shift $t_\gamma = \gamma/\omega_R$, the signal at time $\tau$ is given by

$$s(\tau, \gamma) = Tr[TU(\tau + t_\gamma, t_\gamma)\rho(0)U^+(\tau + t_\gamma, t_\gamma)], \quad [28]$$

where $U(t, 0)$ is the propagator evaluated for $\gamma = 0$. The notation $\rho(0)$ is used because the initial state is often independent of $t_\gamma$ ($\rho(0) = I_Z$ or $I_X$). Extension to the case $\rho(t_\gamma)$ will be described elsewhere (*36*). By expanding $U(\tau + t_\gamma, t_\gamma)$ as in Eq. [7], Eq. [28] can be transformed into

$$s(\tau, \gamma) = Tr[F^+(\tau + t_\gamma)TF(\tau + t_\gamma) \times e^{-i\bar{\Omega}\tau} F^+(t_\gamma)\rho(0)F(t_\gamma)e^{+i\bar{\Omega}\tau}]. \quad [29]$$

We collect the factors in a way which allows to define the new time-dependent periodic observables $\tilde{T}(t)$ and $\tilde{\rho}(t)$ according to the transformation

$$A \Rightarrow \tilde{A}(t) = F^+(t) A F(t). \quad [30]$$

The signal Eq. [29] is then

$$s(\tau, \gamma) = Tr[\tilde{T}(\tau + t_\gamma)e^{-i\bar{\Omega}\tau}\tilde{\rho}(t_\gamma)e^{+i\bar{\Omega}\tau}]. \quad [31]$$

Thus, the observables are transformed into a time-dependent frame where the time-dependent Hamiltonian has been reduced to the time-independent average Hamiltonian $\bar{\Omega}$. As previously mentioned, this transformation is in fact similar to the canonical transformation (*29, 31*), as $F(t)$ can also be expressed as

$$F(t) = e^{-iS(t)}, \quad [32]$$

where $S(t)$ is periodic and unitary.

Introducing the Fourier transform $\tilde{A}_p$ of $\tilde{A}(t)$,

$$\tilde{A}_p = \frac{1}{T_R}\int_0^{T_R} \tilde{A}(t) e^{-ip\omega_R t} dt, \quad [33]$$

the signal can be Fourier expanded with respect to $t$ and $\gamma$, giving

$$s(\tau, \gamma) = \sum_{p,q} Tr[\tilde{T}_p e^{-i\bar{\Omega}\tau}\tilde{\rho}_q e^{+i\bar{\Omega}\tau}] e^{ip\omega_R t} e^{i(p+q)\gamma}. \quad [34]$$

Expanding the trace ($\bar{\Omega}$ is diagonal) and introducing the notation

$$\langle\tilde{A}(t)\rangle_{rs} = \langle r|\tilde{A}(t)|s\rangle \quad [35a]$$

$$\langle\tilde{A}_p\rangle_{rs} = \langle r|\tilde{A}_p|s\rangle \quad [35b]$$

$$\bar{\omega}_{rs} = \langle r|\bar{\Omega}|r\rangle - \langle s|\bar{\Omega}|s\rangle, \quad [35c]$$

one gets

$$s(\tau, \gamma) = \sum_{\substack{p,q \\ r,s}} \langle\tilde{T}_p\rangle_{rs}\langle\tilde{\rho}_q\rangle_{sr} e^{i(p\omega_R + \bar{\omega}_{rs})\tau} e^{i(p+q)\gamma}. \quad [36]$$

The average over the Euler angle can then be carried out analytically and leads to

$$s(\tau) = \frac{1}{2\pi}\int_0^{2\pi} s(\tau, \gamma)d\gamma$$

$$= \sum_{\substack{p \\ r,s}} \langle \tilde{T}_p\rangle_{rs}\langle\tilde{\rho}_{-p}\rangle_{sr} e^{i(p\omega_R + \bar{\omega}_{rs})\tau}. \quad [37]$$

The spectrum $s(\omega)$ of $s(t)$ is then calculated according to

$$s(\bar{\omega}_{rs} + p\omega_R) = \langle \tilde{T}_p\rangle_{rs}\langle\tilde{\rho}_{-p}\rangle_{sr}. \quad [38]$$

Thus, the present approach allows a generalization of the formal average over $\gamma$ to a Hamiltonian which does not commute with itself at different times. To our knowledge, this result has never been reported. It can reduce significantly the overall computing time in MAS, nutation or spin locking simulations (*21–24*). Furthermore, when $\rho(0) = T^+$, using $(\tilde{T}_p)^+ = \tilde{T}^+_{-p}$, the product $\langle \tilde{T}_p\rangle_{rs}\langle\tilde{\rho}_{-p}\rangle_{sr} = |\langle\tilde{T}_p\rangle_{rs}|^2$ is real. This result is known in the case of MAS spectra (*37*). Here it is generalized to the non-self-commuting Hamiltonians which have the property

$$H(\gamma, t) = H(0, t + \gamma/\omega_R). \quad [39]$$

To conclude this section, we give the general method to perform one simulation:

1. The propagator $U(t_j, 0)$ is calculated over a single period (Eq. [11]).
2. $U(T_R)$ is diagonalized to generate the diagonal representation of average Hamiltonian $\bar{\Omega}$ and $F(0)$ (Eq. [9]).
3. The components $F(t_j)$ are evaluated (Eq. [10]).
4. All the required operators $\tilde{A}(t)$ are calculated (Eq. [30]) and Fourier transformed (Eq. [33]).
5. The spectrum $s(\omega)$ is calculated (Eq. [38]).
6. The powder average is calculated by repeating steps 1 to 5 for different $\alpha$, $\beta$ values.
7. If needed, inverse Fourier transform gives $s(\tau)$.

## V. EXTENSION TO COMPLEX SEQUENCES

For a single evolution time, the formalism developed in the preceding sections allows computation of a signal averaged over the angle $\gamma$. When complex sequences such as multipulse applied synchronously with the rotation of the sample are considered, the computation of the signal for each value of $\gamma$ and the summation can be unavoidable. Nevertheless, for calculating the propagator for each angle $\gamma$, we can take advantage of the calculated operator $F(t)$ for the previous values of $\gamma$. For example, let us consider that one period of evolution can be described as a succession of different Hamiltonians $H_A(t)$, $H_B(t)$, $H_C(t)$, ... that have the property Eq. [39]. The computation of the propagator $U^\gamma(t, 0)$ is performed using the recursive method, thus requiring propagators such as $U_X^\gamma(t_j, t_k)$ for each Hamiltonian $H_X(t)$. Following the approach of Section 2, we can use the relation

$$U_X^\gamma(t_k, t_j) = F_X(t_k + \gamma/\omega_R)e^{-i\bar{\Omega}_X(t_k - t_j)}F_X^+(t_j + \gamma/\omega_R) \quad [40]$$

to compute the propagator for the next value of $\gamma$. It is nevertheless still possible to use Eq. [40] in a general trace calculation. By Fourier expansion of the operators $F_X(t + \gamma/\omega_R)$, and change in the various summation indices, it is always possible to get a formal average over $\gamma$. Calculations can be long and rather tedious, but remain straightforward.

## VI. APPLICATION TO QUADRUPOLAR NUCLEI: ROTATIONAL INDUCED ADIABATIC TRANFER OF COHERENCE OF SPIN 3/2

We apply the formalism developed in the previous section to the spin locking of a spin 3/2 in MAS experiment. As pointed out by A. J. Vega (*2, 3*), the rotation at the magic angle induces a time dependence to the first-order quadrupole interaction which results in several zero crossings. Depending on the passage range from slow (adiabatic) to sudden and under several special experimental conditions (on-resonance irradiation), an efficient adiabatic conversion of triple quantum coherence to single quantum coherence can be achieved (*4*).

Here, we consider a spin system consisting of half-integer spin nuclei that are subjected to quadrupole interactions and to a radio-frequency field $\omega_{RF}$. In the conventional rotating frame the Hamiltonian is given by

$$H(t) = H_Q^{(1)}(t) + H_Q^{(2)}(t) + \delta I_z + \omega_{RF} I_X, \quad [41]$$

where $\delta$ is the offset and $H_Q^{(1)}(t)$ and $H_Q^{(2)}(t)$ are the first- and second-order quadrupole interactions. Let us consider a single crystallite described by a Euler angle $\Omega_{CR} = (\alpha, \beta, \gamma)$ in the rotor fixed axes system, which is related to the laboratory fixed axis system by the time-dependent Euler angle $\Omega_{RL} = (\omega_R t, \theta_m, 0)$, where $\theta_m = 54.74°$ is the magic angle. The Hamiltonian can be expanded as

$$H(\alpha, \beta, \gamma, t) = \sum_m H_m(\alpha, \beta)e^{im(\omega_R t + \gamma)}. \quad [42]$$

Introducing the parameter $\theta = \omega_R t + \gamma$, we obtain

$$H(\alpha, \beta, \theta) = \sum_m H_m(\alpha, \beta)e^{im\theta}. \quad [43]$$

The evolution operator is

$$U^\gamma(t, 0) = \hat{T}\exp\left(-\frac{i}{\omega_R}\int_\gamma^{\omega_R t + \gamma} H(\alpha, \beta, \theta)d\theta\right). \quad [44]$$

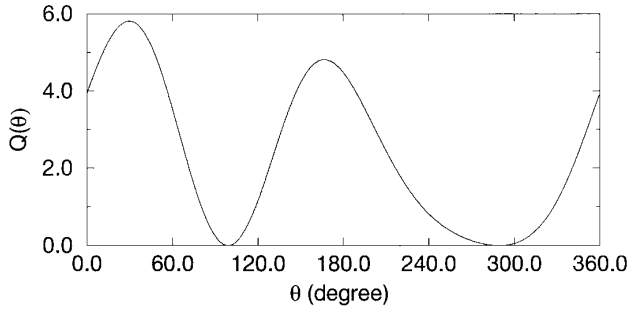


**FIG. 1.** For $^{23}$Na in $Na_2C_2O_4$, $\theta$-dependence of the relative quadrupolar strength $Q(\theta)$ (Eq. [48]). The crystallite orientation in the rotor fixed frame is $\Omega_{CR} = (\alpha = 30°, \beta = 60°, \theta)$.

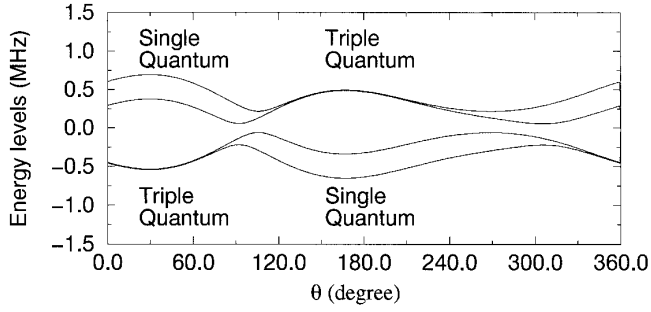


**FIG. 2.** For $^{23}$Na in $Na_2C_2O_4$, $\theta$-dependence of the energy levels of $H(\alpha, \beta, \theta)$ (Eq. [43]); same crystallite orientation as in Fig. 1.

To describe the RIACT, we calculate the signal

$$s^{\gamma}(t) = Tr[I_{-}^{2,3} U^{\gamma}(t, 0) I_{+}^{1,4} U^{\gamma+}(t, 0)], \qquad [45]$$

where the matrix representation of the single and triple quantum fictitious spin operators (*38–40*) is

$$I_{+}^{1,4} = \begin{pmatrix} 0 & 0 & 0 & 1 \\ 0 & 0 & 0 & 0 \\ 0 & 0 & 0 & 0 \\ 0 & 0 & 0 & 0 \end{pmatrix}, I_{-}^{2,3} = \begin{pmatrix} 0 & 0 & 0 & 0 \\ 0 & 0 & 0 & 0 \\ 0 & 1 & 0 & 0 \\ 0 & 0 & 0 & 0 \end{pmatrix}. \qquad [46]$$

For a single crystallite, we will compare the accuracy of the three following methods: the recursive method, Floquet space calculation, and the present method.

An estimation of the accuracy is obtained by choosing as a reference signal $s_{\mathrm{REF}}(t)$ (obtained by the recursive method with a discretization of the rotation in 1024 steps) and computing the function

$$\frac{\int_0^{T_R} |s(t) - s_{\mathrm{REF}}(t)|^2 dt}{\int_0^{T_R} |s_{\mathrm{REF}}(t)|^2 dt}. \qquad [47]$$

The calculations are performed using the quadrupolar parameters of $^{23}$Na in $Na_2C_2O_4$ ($e^2qQ/h = 2.6$ MHz, $\eta = 0.7$) and the experimental conditions $\omega_{RF} = 160$ kHz, $\delta = 3$ kHz, $\omega_R = 12.5$ kHz. Figure 1 displays the angular dependence of the relative strength of the quadrupole interaction taken as

$$Q(\theta) = \frac{Tr[H_Q^{+}(\theta) H_Q(\theta)]}{\omega_Q^2}, \qquad [48]$$

where $H_Q(\theta) = H_Q^{(1)}(\theta) + H_Q^{(2)}(\theta)$ and $\omega_Q = e^2qQ/2I(2I-1)h$. Two limiting cases can be distinguished. When $Q(\theta) \gg \omega_{RF}/\omega_Q$, taking into account only the isotropic part of $H_Q^{(2)}(\theta)$ (i.e., $\bar{H}_Q^{(2)} = \delta_Q^{2,3} I_Z^{2,3} + \delta_Q^{1,4} I_Z^{1,4}$), diagonalization to first order gives the approximation by keeping only the meaningful terms (*42*),

$$H(\theta) \approx \omega_Q V_{20}(\theta) T_{20} + 2\omega_{RF} I_X^{2,3} + \omega_X^{1,4} I_X^{1,4} + (\delta + \delta_Q^{1,4}) I_Z^{1,4} \qquad [49a]$$

$$\approx \omega_Q V_{20}(\theta) T_{20} + 2\omega_{RF} I_X^{2,3} + \omega_\phi^{1,4} I_\phi^{1,4}, \qquad [49b]$$

where $\omega_X^{1,4} \propto \omega_{RF}^3/\omega_Q^2$. The Hamiltonian is expanded into three constants of motion, that is, parts that commute with one another. The eigensystem can be viewed as being divided in a triple quantum subset, polarized along the direction defined by the angle $\phi$ in the $(X, Z)$ plane, and a single quantum subset polarized along $X$. When $Q(\theta) \ll \omega_{RF}/\omega_Q$, the Hamiltonian is mainly given by

$$H(\theta) \approx \omega_{RF} I_X. \qquad [50]$$

The energy levels can be seen in Fig. 2, $I_\phi^{1,4}$ corresponding to an almost degenerate subset when the offset is small compared to $\omega_X^{1,4}$. The anticrossing of the levels results in the periodical transformation of the subset from $I_X^{2,3}$ to $I_\phi^{1,4}$. Hence, if the passage is sufficiently slow, the system which is originally in an eigenstate of the Hamiltonian will pass into the eigenstate derived from it by continuity. Under these conditions, one can transfer the triple quantum into the single quantum coherence.

Figure 3 gives the reference signal, Eq. [45], for a crystallite. Figures 4 and 5 display the error function Eq. [47] with respect to

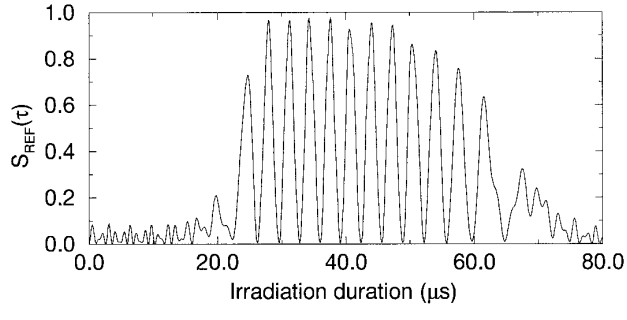


**FIG. 3.** For $^{23}$Na in $Na_2C_2O_4$, signal intensity $s_{\mathrm{REF}}(t)$ (Eq. [45]). The crystallite orientation is $\Omega_{CR} = (\alpha = 30°, \beta = 60°, \gamma = 0°)$ and the parameters are $\omega_R = 12.5$ kHz, $\omega_{RF} = 160$ kHz, $\delta = 3$ kHz. The rotation period is discretized in 1024 steps.

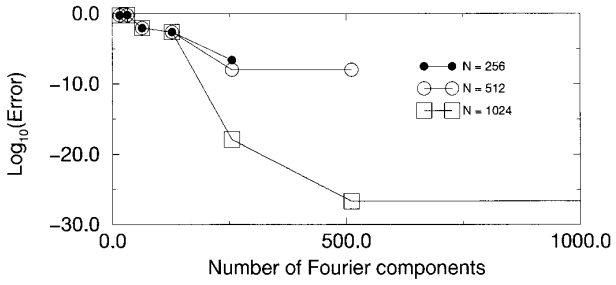


**FIG. 4.** For $^{23}$Na in $Na_2C_2O_4$, dependence of the error function Eq. [47] for different discretizations of the rotation period in $N$ steps, with same NMR parameters as in Fig. 3.

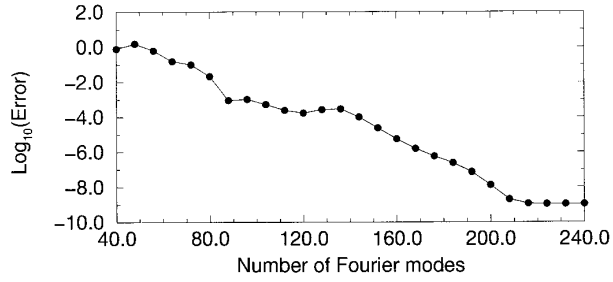


**FIG. 5.** For $^{23}$Na in $Na_2C_2O_4$, dependence of the error function Eq. [47] on the number of Fourier modes in Floquet space calculation, with same NMR parameters as in Fig. 3.

the discretization parameter with the present method and with Floquet space calculations, respectively. An error less than $10^{-8}$ gives a curve than cannot be distinguished from the reference curve. Thus, sufficient accuracy is obtained with a discretization in 256 steps of the rotation for evaluating the $U(t_j, 0)$ operators and 256-mode Fourier components. For the Floquet space approach, more than 200 mode states are required. These values are of the same order as expected from the relation Eq. [26]. The CPU time needed[2] for the diagonalization of the Floquet Hamiltonian was 302.25 s, whereas by the present method, evaluation of the $\bar{\Omega}$ and $F_n$ operators required 0.11 s.

Agreement of our simulation with experiment for powder signals is shown in Fig. 6 for short pulses and in Fig. 7 for long on-resonance irradiation. The experimental data were acquired using a hypercomplex phase cycling (*43*) and we plot the area of the spectra for different pulse widths of the second pulse which transfer the triple quantum coherence into the single one. Nevertheless, for pulse width greater than 6 $\mu$s, a loss of half of the signal was observed during the first quarter of the rotation period as shown in Fig. 6. In Fig. 7, the theoretical curve was scaled by a factor of 2 with respect to the theoretical curve of Fig. 6. Considering all the preparation period, that is, the excitation of the triple quantum coherence before its conversion, does not lead to any significant modification of our theoretical result. The signal is simply scaled. We also tried to take into account some local field $\delta I_Z$ with a Gaussian distribution of the parameter $\delta$. This could not reproduce so rapid a loss of signal during the first quarter-period. This phenomenon is unexplained for the moment, and other models are currently being investigated, such as taking into account the homonuclear dipolar interaction by considering several spins. This interaction is not crucial in the hard pulse regime but can have a significant effect in the adiabatic conversion process. Nevertheless, the good agreement of our simulation with the experimental data for long irradiation shows that the model is reliable for describing the RIACT phenomenon. The critical dependence with respect to the offset in the adiabatic conversion process is shown in Fig. 8, where the signal is computed for an optimal short pulse duration (3 $\mu$s) and one-quarter of the rotation period (20 $\mu$s). It is also visible in the powder averaged spectra (Fig. 9) that the intense components at multiples of the rotation frequency disappear when the offset increases. These well-resolved components at the rotation frequency lead us to conclude that some part of the triple quantum coherence and the single quantum coherence are locked to multiples of the rotation frequency under on-resonance irradiation. Such considerations can be of great interest in studying the possibility of locking the triple quantum coherence for multiple quantum cross-polarization processes. This will be further investigated.

## VII. CONCLUSION

Some properties of the evolution operator for periodic time-dependent Hamiltonians have been carefully analyzed. This allows significant improvements in the calculation of the response of spin systems in sample-spinning NMR experiments. That simulation method is more efficient than the Floquet space method,

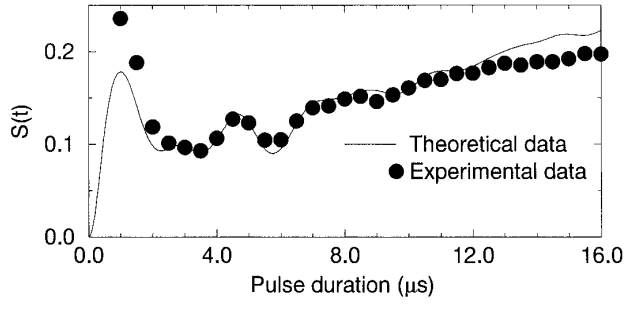


**FIG. 6.** For $^{23}$Na in $Na_2C_2O_4$, experimental and simulated powder signal Eq. [45] with respect to pulse duration in microseconds. Experimental data were obtained on a Bruker 300-Mhz DMX with $\omega_R = 12.5$ kHz, $\omega_{RF} = 160$ kHz, $\delta = 3$ kHz. For numerical data, the rotation is discretized in 256 steps.

[2] Calculations were performed on an UltraSparc II (CPU frequency 170 MHz) SUN station with a program written in FORTRAN 90, using the diagonalization procedures F02HAF and F02GBF of the NAG FORTRAN library (mark 16).

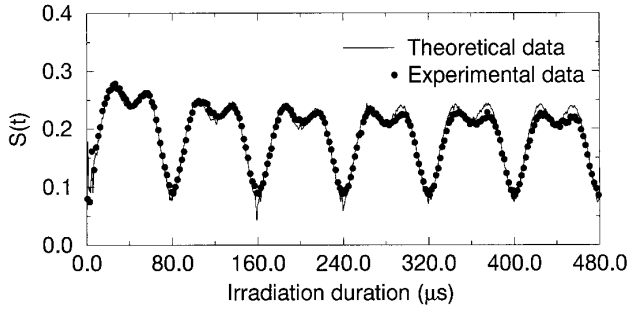


**FIG. 7.** For $^{23}Na$ in $Na_2C_2O_4$, experimental and simulated powder signal Eq. [45] with respect to on-resonance irradiation duration in microseconds, with same NMR parameters as in Fig. 6.

which requires diagonalization of a matrix of large dimension. Moreover, that method can be seen as a new way of diagonalizing the Floquet matrix by taking advantage of its band structure. Generalization of our approach for multimode is currently being investigated. The application to the complete simulation of MQ-MAS spectra (*44*, *45*), including the Z-filtering method (*46*), will be presented elsewhere (*36*). This approach will also be useful in theoretical studies of CPMAS processes for quadrupolar nuclei. Research in this direction is being undertaken.

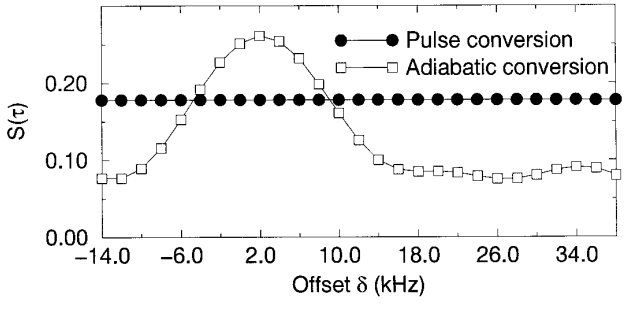


**FIG. 8.** For $^{23}Na$ in $Na_2C_2O_4$, theoretical dependence of the powder signal intensity Eq. [45] on the offset (a) for small pulse width ($\tau = 3\ \mu s$) and (b) for adiabatic conversion ($\tau = 20\ \mu s$) with the same parameters as Fig. 6.

## APPENDIX A

The evolution operator in the Floquet space is

$$U^F(t, 0) = e^{-iH^F t} = W^F e^{-i\bar{\Omega}^F t} W^{F+}. \qquad [A1]$$

The eigenvalues of the Floquet Hamiltonian are known to be of the form

$$\lambda_n^i = \lambda_0^i + n\omega_R, \qquad [A2]$$

where $i$ indexes the spin state and $n$ the Floquet mode. Thus, introducing the block matrix

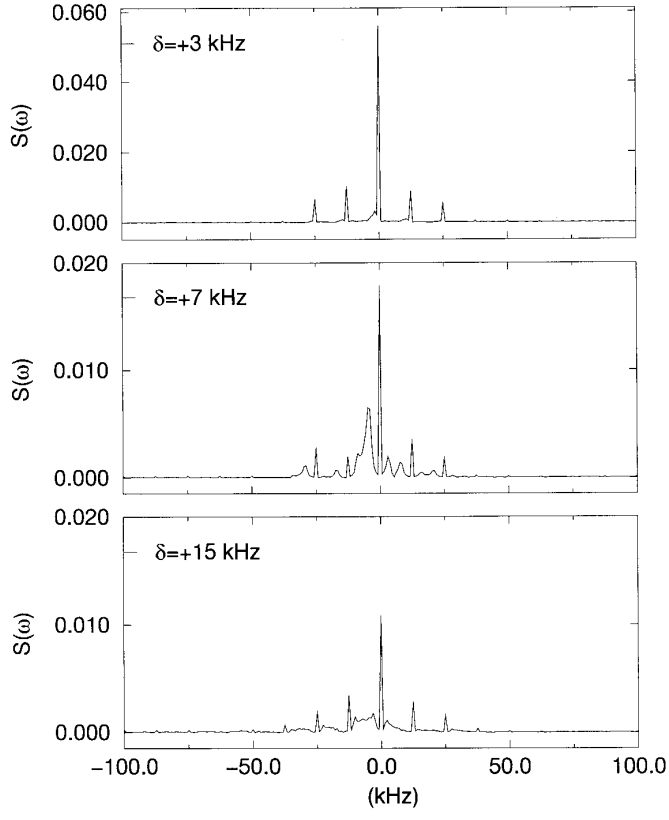


**FIG. 9.** For $^{23}Na$ in $Na_2C_2O_4$, spectra $s(\omega)$ (Eq. [38]) of the powder signal for different values of the offset, other parameters being the same as in Fig. 6.

$$N^F = \sum_k k|k\rangle\langle k| = \begin{pmatrix} \cdots & \cdots & \cdots & \cdots & \cdots \\ \cdots & -\mathrm{Id} & 0 & 0 & \cdots \\ \cdots & 0 & 0 & 0 & \cdots \\ \cdots & 0 & 0 & +\mathrm{Id} & \cdots \\ \cdots & \cdots & \cdots & \cdots & \cdots \end{pmatrix}. \qquad [A3]$$

and

$$I^F = \sum_k |k\rangle\langle k|, \qquad [A4]$$

$\bar{\Omega}^F$ can be rewritten as $\bar{\Omega} = \omega_R N^F + \bar{\Omega} I^F$. We want to derive the equivalence between Eqs. [21] and [22]. We recall some useful properties:

$$\sum_n \langle n|\Phi^F(0)\rangle = \mathrm{Id} \qquad [A5a]$$

$$e^{-i\omega_R N^F t}|k\rangle = e^{-ik\omega_R t}|k\rangle \qquad [A5b]$$

$$e^{-i\bar{\Omega} I^F t}|k\rangle = e^{-i\bar{\Omega} t}|k\rangle \qquad [A5c]$$

$$\langle p + k|W^F|k\rangle = \langle p|W^F|0\rangle. \qquad [A5d]$$

Equation [21] can be transformed as follows:

$$\begin{aligned} U(t,0) &= \sum_{n,k} \langle n|e^{-iH^F t}|k\rangle\langle k|\Phi^F(0)\rangle e^{in\omega_R t} \\ &= \sum_{n,k,p} \langle n|W^F|p\rangle \langle p|e^{-i\bar{\Omega}^F t}|p\rangle \langle p|W^{F+}|k\rangle \langle k|\Phi^F(0)\rangle e^{in\omega_R t} \\ &= \sum_{n,k,q} \langle n|W^F|q+k\rangle e^{-i(q+k)\omega_R t} e^{-i\bar{\Omega}t} \langle q+k|W^{F+}|k\rangle \\ &\quad \times \langle k|\Phi^F(0)\rangle e^{in\omega_R t}. \end{aligned} \quad [A6]$$

Applying the band structure property Eq. [A5d] leads to the final result,

$$\begin{aligned} U(t,0) &= \sum_{n,k,q} \langle n-k|W^F|q\rangle e^{-iq\omega_R t} e^{-i\bar{\Omega}t} \langle q|W^{F+}|0\rangle \\ &\quad \times \langle k|\Phi^F(0)\rangle e^{i(n-k)\omega_R t} \\ &= \sum_{m,q} \langle m|W^F|q\rangle e^{-iq\omega_R t} e^{-i\bar{\Omega}t} \langle q|W^{F+}|0\rangle \\ &\quad \times \sum_k \langle k|\Phi^F(0)\rangle e^{im\omega_R t} \\ &= \sum_m \langle m|e^{-iH^F t}|0\rangle e^{im\omega_R t}. \end{aligned} \quad [A7]$$

## APPENDIX B

Using the method of Appendix A, $V_n(t) = \langle n|e^{-iH^F}t|0\rangle$ can be expanded as

$$V_n(t) = \sum_k \langle n|W^F|k\rangle e^{-i\bar{\Omega}t} \langle k|W^{F+}|0\rangle e^{-ik\omega_R t}. \quad [B1]$$

The band structure and Eq. [26] (derived in Appendix C) give

$$V_n(t) = \sum_k F_{n-k} e^{-i\bar{\Omega}t} F_k^+ e^{-ik\omega_R t}. \quad [B2]$$

Inserting $F(0)F^+(0) = \mathrm{Id}$, we obtain

$$V_n(t) = \sum_k U_{n-k}(t) U_k^+(0) e^{-ik\omega_R t}, \quad [B3]$$

which shows that the Fourier coefficients of Eq. [22] $V_n(t)$, are oscillating quickly.

## APPENDIX C

From Eq. [22], using the same method as in Appendix A (Eqs. [A6] and [A7]), we obtain

$$\begin{aligned} U(t,0) &= \sum_{k,n} \langle n|W^F|k\rangle e^{-i\bar{\Omega}t} \langle k|W^{F+}|0\rangle e^{i(n-k)\omega_R t} \\ &= \sum_{k,p} \langle p+k|W^F|k\rangle e^{-i\bar{\Omega}t} \langle k|W^{F+}|0\rangle e^{ip\omega_R t} \\ &= \left(\sum_p \langle p|W^F|0\rangle e^{ip\omega_R t}\right) e^{-i\bar{\Omega}t} \left(\sum_k \langle k|W^{F+}|0\rangle\right). \end{aligned} \quad [C1]$$

Comparison with Eq. [7] leads to

$$F_p = \langle p|W^F|0\rangle. \quad [C2]$$

It should be mentioned that the initial state $|\Phi^F(0)\rangle$, Eq. [19], is related to the usual initial state $|0\rangle$ by

$$|\Phi^F(0)\rangle = W^F F^+(0)|0\rangle. \quad [C3]$$

*Note added in proof.* The formal average over $\gamma$ (Eqs. [38] and [39]) was recently proposed within the COMPUTE formalism by M. H. Levitt and M. Edén in the paper ''Numerical Simulation of Periodic NMR Problems: FAST Calculation of Carousel Averages,'' submitted to *Mol. Phys.*

## REFERENCES


1. M. Eden, Y. K. Lee, and M. H. Levitt, *J. Magn. Reson. A* **120,** 56 (1996).
2. A. J. Vega, *Solid State NMR* **1,** 17 (1992).
3. A. J. Vega, *J. Magn. Reson.* **96,** 50 (1992).
4. G. Wu, D. Rovnyak, and R. G. Griffin, *J. Am. Chem. Soc.* **118,** 9326 (1996).
5. H. Sambe, *Phys. Rev. A* **7,** 2203 (1073).
6. D. Moore, *J. Phys. A* **23,** L665 (1990).
7. J. H. Shirley, *Phys. Rev. B* **138,** 1979 (1065).
8. T. S. Ho and S. I. Chu, *Chem. Phys. Lett.* **122,** 327 (1985).
9. T. S. Ho, K. Wang, and S. I. Chu, *Phys. Rev. A* **33,** 1798 (1986).
10. K. Wang and S. I. Chu, *J. Chem. Phys.* **86,** 3225 (1987).
11. S. I. Chu, *Adv. Chem. Phys.* **73,** 739 (1989).
12. S. I. Chu, *Radiat. Effects. Defects. Solids.* **122–123,** 57 (1991).
13. T. O. Levante, M. Baldus, B. H. Meier, and R. R. Ernst, *Mol. Phys.* **86,** 1195 (1995).
14. T. Nakai and C. A. McDowell, *J. Chem. Phys.* **96,** 3452 (1992).
15. T. Nakai and C. A. McDowell, *Mol. Phys.* **88,** 1263 (1996).
16. A. Schmidt and S. Vega, *J. Chem. Phys.* **87,** 6895 (1987).
17. A. Schmidt and S. Vega, *J. Chem. Phys.* **96,** 2652 (1992).
18. D. Marks and S. Vega, *J. Magn. Reson. A* **118,** 157 (1995).
19. S. Hediger, B. H. Meier, and R. R. Ernst, *J. Chem. Phys.* **102,** 4000 (1995).
20. S. Hediger, P. Signer, M. Tomaselli, and R. R. Ernst, *J. Magn. Reson.* **125,** 291 (1997).
21. W. Sun, J. T. Stephen, L. D. Potter, and Y. Wu, *J. Magn. Reson. A* **116,** 181 (1995).
22. N. C. Nielsen, H. Bildsøe, and H. J. Jakobsen, *J. Magn. Reson.* **97,** 149 (1992).
23. S. Ding and C. A. McDowell, *J. Magn. Reson. A* **112,** 36 (1995).

*24.* N. C. Nielsen, H. Bildsøe, and H. J. Jakobsen, *Chem. Phys. Lett.* **191,** 205 (1992).

*25.* D. Marks, N. Zumbulyadis, and S. Vega, *J. Magn. Reson. A* **120,** 16 (1996).

*26.* U. Haeberlen and J. S. Waugh, *Phys. Rev.* **175,** 453 (1968).

*27.* U. Haeberlen, ''High Resolution NMR in Solids.'' Academic Press, New York (1976).

*28.* M. Mehring, ''Principles of High Resolution NMR in Solids,'' 2nd Ed. Springer-Verlag, Berlin (1983).

*29.* A. Llor, *Chem. Phys. Lett.* **199,** 383 (1992); A. Llor, *Chem. Phys. Lett.* **204,** 217 (1993).

*30.* G. Floquet, *Ann. Ec. Norm. Sup.* **12,** 47 (1883).

*31.* B. N. Provotorov and É. B. Fel'dman, *Sov. Phys. JEPT* **52,** 1116 (1980).

*32.* W. Zhu and X. Zhao, *J. Chem. Phys.* **105,** 9536 (1996).

*33.* O. Weintraub and S. Vega, *J. Magn. Reson. A* **105,** 245 (1993).

*34.* O. Weintraub, S. Vega, Ch. Hoelger, and H. H. Limbach, *J. Magn. Reson. A* **109,** 14 (1994).35.

*35.* D. Abramovich, S. Vega, J. Quant, and S. J. Glaser, *J. Magn. Reson. A* **115,** 222 (1995).

*36.* T. Charpentier, C. Fermon, and J. Virlet, unpublished.

*37.* M. H. Levitt, *J. Magn. Reson.* **82,** 427 (1989).

*38.* S. Vega and A. Pines, *J. Chem. Phys.* **66,** 5624 (1977).

*39.* A. Wokaun and R. R. Ernst, *J. Chem. Phys.* **67,** 1752 (1977).

*40.* S. Vega, *J. Chem. Phys.* **68,** 5518 (1978).

*41.* S. Vega and Y. Naor, *J. Chem. Phys.* **75,** 75 (1981).

*42.* S. Vega, *Phys. Rev. A* **23,** 3152 (1981).

*43.* D. Massiot, B. Touzo, D. Trumeau, J. P. Couture, J. Virlet, P. Florian, and P. J. Grandinetti, *Solid State NMR* **6,** 73 (1996).

*44.* L. Frydman and J. S. Harwood, *J. Am. Chem. Soc.* **117,** 5367 (1995).

*45.* A. Medek, J. S. Harwood, and L. Frydman, *J. Am. Chem. Soc.* **117,** 12779 (1995).

*46.* J. P. Amoureux, C. Fernandez, and S. Steuernagel, *J. Magn. Reson. A* **123,** 116 (1996).